

A high-throughput direct FRET-based assay for analysing apoptotic proteases using flow cytometry and fluorescence-lifetime measurements

Miho Suzuki, Ichiro Sakata, Takafumi Sakai, Hiroaki Tomioka, Koichi Nishigaki, Marc Tramier, Maïté Coppey-Moisan

▶ **To cite this version:**

Miho Suzuki, Ichiro Sakata, Takafumi Sakai, Hiroaki Tomioka, Koichi Nishigaki, et al.. A high-throughput direct FRET-based assay for analysing apoptotic proteases using flow cytometry and fluorescence-lifetime measurements. Analytical Biochemistry, 2015, 491, pp.10-17. 10.1016/j.ab.2015.08.022 . hal-01196602

HAL Id: hal-01196602

https://univ-rennes.hal.science/hal-01196602

Submitted on 2 Dec 2015

HAL is a multi-disciplinary open access archive for the deposit and dissemination of scientific research documents, whether they are published or not. The documents may come from teaching and research institutions in France or abroad, or from public or private research centers.

L'archive ouverte pluridisciplinaire **HAL**, est destinée au dépôt et à la diffusion de documents scientifiques de niveau recherche, publiés ou non, émanant des établissements d'enseignement et de recherche français ou étrangers, des laboratoires publics ou privés.

ACCEPTED MANUSCRIPT

A high-throughput direct FRET-based assay for analysing apoptotic proteases using flow cytometry and fluorescence-lifetime measurements

Miho Suzuki[a*], Ichiro Sakata[b], Takafumi Sakai[b], Hiroaki Tomioka[c], Koichi Nishigaki[a], Marc Tramier[d], Maïté Coppey-Moisan[e]

[a] Department of Functional Materials and Science, Graduate School of Science and Engineering, Saitama University, Saitama, Japan

[b] Department of Regulatory Biology, Graduate School of Science and Engineering, Saitama University, Saitama, Japan

[c] Department of Science Education, Graduate School of Education, Saitama University, Saitama, Japan

[d] Institut de Génétique et Développement de Rennes, UMR 6290, CNRS, Université Rennes 1, Rennes, France

[e] Institut Jacques Monod, Complexes Macromoléculaires en Cellules Vivantes, UMR 6290, CNRS, Université Paris-Diderot, Paris, France

*Corresponding author: Miho Suzuki, Email: miho@fms.saitama-u.ac.jp, Tel/Fax: +81-48-858-3533.

Short Title

FRET assay for proteases by flow cytometry

ACCEPTED MANUSCRIPT

ACCEPTED MANUSCRIPT

Abstract

Cytometry is a versatile and powerful method applicable to different fields, particularly pharmacology and biomedical studies. Based on the data obtained, cytometric studies are classified into high-throughput (HTP) or high-content screening (HCS) groups. However, assays combining the advantages of both are required to facilitate research. In this study, we developed a high-throughput system to profile cellular populations in terms of time- or dose-dependent responses to apoptotic stimulations, since apoptotic inducers are potent anti-cancer drugs. We previously established assay systems involving protease to monitor live cells for apoptosis using tuneable FRET-based bioprobes. These assays can be used for microscopic analyses or fluorescence-activated cell sorting. In this study, we developed FRET-based bioprobes to detect the activity of the apoptotic markers caspase-3 and caspase-9 via changes in bioprobe fluorescence lifetimes using a flow cytometer for direct estimation of FRET efficiencies. Different patterns of changes in the fluorescence lifetimes of these markers during apoptosis were observed, indicating a relationship between discrete steps in the apoptosis process. The findings demonstrate the feasibility of evaluating collective cellular dynamics during apoptosis.

Keywords: FRET; fluorescence lifetime; apoptosis; flow cytometry; high-throughput assay

ACCEPTED MANUSCRIPT

ACCEPTED MANUSCRIPT

1. Introduction

Cell-based assays are essential components of drug development and medicinal studies; these assays generally succeed *in vitro* experiments and precede animal trials [1–3]. Various assays have been developed to obtain additional information regarding cellular function; however, standardization and integration of data obtained from these assays present a challenge due to the variation between these assays. Depending on the instrumentation system used, these assays are static or dynamic, statistical or individual, and comprehensive (encompassing a range of measurements and observation targets) or focused. In this study, we developed a functionally-merged, customized cell-based assay that could facilitate drug discovery and basic omics studies. Flow cytometers are devices generally used in high-throughput (HTP) screening assays analysing heterogeneous cell populations [4–6]. Detection of specific intracellular or cell-surface components using a flow cytometer mainly relies on fluorescence, introduced by labelling the components (of interest) with a fluorophore. Static multi-index evaluation systems have also been established for the promotion of basic and clinical research [7–9]. Alternatively, high-content screening (HCS) for cell-based assays facilitates cellular-imaging analysis with high spatial resolution [10–13]. In HCS, carefully designed sensing molecules are introduced into the cells to enable quantitative evaluation of the conditions within each cell. These evaluations are performed using imaging cytometers or microplate readers developed specifically for this purpose [10–13].

In this study, we combined the advantages of both, HTP and HCS, thus integrating cellular dynamic

ACCEPTED MANUSCRIPT

characterization with authentic high-throughput analysis in the context of cell population profiling. In addition to the applicable equipment, we used fluorescence resonance energy transfer (FRET)-based chimeric sensing molecules, known as chimeric FRET bioprobes [14, 15]. All analyses were performed using a flow cytometer designed to measure fluorescence lifetimes. This device allowed for rapid, sensitive, and statistical measurement of the average fluorescence lifetime of a cellular population (several thousand cells per second, lifetime accuracy ≈ 0.02 ns), in the presence of adequate optical filters. FRET-based analyses are generally used to determine changes in fluorescence intensities of all components of the relevant sensing molecules, in order to quantify targets [16–18]. While the apparent changes in fluorescence intensities must be calibrated in order to estimate the net change in fluorescent properties of all components in some cases, other cases require an elaborate technological setup [19–21].

Fluorescence lifetimes of the energy-donor components of FRET pairs reflect the appearance or disappearance of FRET. Systems developed for FRET-based measurement of equivalent performances can be moderately simple and direct [22–26]. Consequently, samples containing FRET-based sensing molecules are judged suitable for HTP fluorescence-lifetime measurements using appropriate apparatus. Numerous attempts have been made to monitor the cellular events using flow cytometry and FRET-based sensing molecules [27–29]; however, these methods have not been exploited or developed chiefly because of the complexity of FRET-based sensing. We have previously fabricated FRET bioprobes for live-cell imaging and common FACS systems [30]. Quantitative analyses of the reaction kinetics of these bioprobes also revealed their functionality

ACCEPTED MANUSCRIPT

as artificial substrates in several systems [14, 31, 32]. The developed FRET bioprobes are chimeric molecules consisting of a donor fluorescent protein and an acceptor organic fluorescent dye. These bioprobes can be used in a wide range of analytical systems because of their ease of handling under *in vitro* and *in vivo* conditions, as well as the ease with which their fluorescent properties can be tuned to conform to specific conditions. In fact, we previously tuned the emission profiles of these bioprobes by selecting appropriate donor and acceptor molecules, allowing for the simultaneous utilization of some bioprobes.

Caspase-3, a key protease affecting apoptosis, was before selected as a FRET bioprobe target [33–35]. Apoptosis, or programmed cell death, involves a complicated signal transduction cascade, which includes the activation of a number of kinases and proteases, and alterations in redox states and membrane potentials [36–38]. Cancer cells display anti-apoptotic conditions [39, 40]; therefore, a number of apoptosis-inducing agents have been reported to function as anti-cancer drugs. On the other hand, anti-apoptotic agents that mitigate neurodegeneration caused by apoptosis are known to prevent the spread of neuronal diseases [41–43]. Therefore, to establish a dynamic system to study the cellular population, we generated a FRET bioprobe for caspase-9, an upstream mediator of caspase-3 activity during apoptosis; the signal transduction properties of caspase-9 were compared to those of caspase-3 [44, 45]. In this study, we also demonstrated the feasibility and future applicability of the FRET bioprobe in an apoptotic protease inhibitor/activator screening assay.

ACCEPTED MANUSCRIPT

2. Material and methods

2.1. Production of green fluorescent protein (GFP) variants for chimeric FRET bioprobes

Mutant GFP was isolated as previously described [30]. Briefly, the previously constructed plasmid pUV5casS22tag, which encodes a GFP derivative for the detection of caspase-3 activity, was transfected into *Escherichia coli* BL21(DE3) (BioDynamics Laboratory Inc., Tokyo, Japan). The transfected bacteria were cultured in Luria-Bertani medium containing 75 μg/mL ampicillin; the expression of the GFP derivative was induced by isopropyl β-D-1-thiogalactopyranoside. The bacteria were harvested and lysed with a sufficient amount of bacterial protein-extraction reagent, B-PER II (Thermo Scientific Pierce, Rockford, IL). The target protein was separated from the lysate via centrifugation and purified by affinity chromatography using a Ni^{2+}-NTA resin; the purified protein was reconstituted in phosphate-buffered saline (PBS) by gel permeation.

A plasmid encoding a different GFP derivative was generated through inverse polymerase chain reaction (PCR). This newly constructed plasmid was based on pUV5casS52tag, where the caspase-3 recognition sequence DEVD was replaced with the caspase-9 recognition sequence LEHD, allowing for the assessment of caspase-9 activity [44-46]. PCR performance was confirmed by ordinal sequencing; the resulting plasmid (pUV5cas12-1) was transfected into *E. coli* BL21(DE3). All subsequent procedures, such as bacterial culture, protein production, extraction, and purification were performed as described above in this section for pUV5casS52. We also verified whether this newly established recognition sequence for caspase-9 functioned with our probes in the same way as for caspase-3 mentioned in the paragraph 2.4.

2.2. Preparation of chimeric FRET bioprobes by modification of GFP variants with fluorescent dyes

Purified fluorescent proteins were chemically modified with various fluorescent dyes such as Alexa Fluor 546, Alexa Fluor 594, Alexa Fluor 750 C_5-maleimide, BODIPY 630/650 methyl bromide, QSY 7 C_5-maleimide (Life Technologies, Carlsbad, CA), or DyLight 680 Maleimide (Thermo Scientific Pierce). The naming convention followed for the resulting complexes was bioprobe-*xx*, for e.g. bioprobe-QSY 7. Appropriate GFP (100 µL of 20 µM solution) was reduced with 1 mM dithiothreitol (DTT) for 10 min at room temperature. Excess DTT was removed by gel filtration (NICK column; GE Healthcare, Buckinghamshire, UK); an aliquot of the eluate (400 µL) was immediately incubated with 2 µL of the corresponding fluorescent dye (10 mg/mL; in dimethyl sulfoxide) at 37°C for 4 h. The resulting solution was subjected to centrifugal filtration (EMD; Millipore Corp., Billerica, MA) in order to remove any unreacted dye and to concentrate it to an appropriate volume for use in subsequent analyses.

2.3. Investigation of fluorescent properties of the FRET bioprobes

The FRET bioprobes were assessed by fluorescence spectroscopy, using a Shimadzu RF-5300PC spectrophotometer (Shimadzu, Kyoto, Japan) at 488 nm (excitation). Fluorescence lifetimes of the FRET bioprobes were determined by confocal time-resolved microscopy, using a MicroTime 200 (PicoQuant GmbH, Berlin, Germany). This microscope is equipped with a picosecond pulse-diode laser that produces an excitatory

ACCEPTED MANUSCRIPT

pulse at 470 nm, as well as a time-correlated single-photon counting (TCSPC) detector (Single Photon Avalanche Diodes; Micro Photon Devices, Bolzano, Italy) coupled to a TimeHarp 300 PC board (PicoQuant GmbH), which is operated in a time-tagged, time-resolved mode. Data acquisition was performed for 1 min at a fixed confocal position in the solution and the data obtained was subsequently fitted to a fluorescence-decay curve using SymPhoTime 64 software (PicoQuant GmBH) to determine lifetimes and proportions of the various components.

2.4. *In vitro* confirmation of freshly introduced bioprobe specificity for caspase-9

We prepared bioprobe-Alexa Fluor 532, 546 and 555 using fluorescent protein UV5cas12-1. 1 unit active caspase-3 (MBL Co. Ltd., Nagoya, Japan) or caspase-9 (Abcam plc, Cambridge, UK) was added to an aliquot of 1 μM of any bioprobe-Alexa Fluor dye solution reconstituted in an assay buffer containing 50 mM 2-[4-(2-hydroxyethyl)piperazin-1-yl] ethanesulfonic acid (HEPES), 50 mM NaCl, 0.1% 3-[(3-cholamidopropyl) dimethylammonio]-1-propanesulfonate (CHAPS) detergent, 10 mM DTT, 5% glycerol, and 10 mM ethylenediaminetetraacetic acid (EDTA), and incubated at 37°C for 2 h. We also arranged similar sample without caspase as a control. Fluorescence spectra for all samples were measured to check caspase-9 specificity by changes in emission ratios [30] (Supplementary Fig. S1) with Jasco Spectrofluorometer, FP-8500 (Jasco Corp., Tokyo, Japan).

ACCEPTED MANUSCRIPT

2.5. *In vitro* monitoring of caspase-3 activity by fluorescence-lifetime analysis

The bioprobe concentration was estimated based on the recovery rate of the preparation process. A solution of bioprobe-Alexa Fluor 546 or bioprobe-Alexa Fluor 750 (approximately 10 μM) was added to an assay buffer containing 20 mM 2,2′-piperazine-1,4-diyldiethanesulfonic acid (PIPES), 100 mM NaCl, 0.1% CHAPS detergent, 10 mM DTT, 10% sucrose, and 1 mM EDTA and incubated at 30°C for 2 h with or without 1 U active caspase-3 to monitor caspase-3 activity. Subsequently, the solution was diluted to an appropriate level and fluorescence-lifetime was measured for each sample.

2.6. Introduction of chimeric FRET bioprobes into HeLa cells s

A solution of the FRET bioprobe (approximately 25 μM) in PBS (30 μL) was added to a tube containing a 3-μL dry film of BioPORTER reagent (Gene Therapy Systems, San Diego, CA). The mixture was hydrated for approximately 10 min at room temperature. The solution was then suspended in 270 μL HyClone Dulbecco's Modified Eagle Medium (DMEM)/High Glucose culture medium (Thermo Fisher Scientific, Massachusetts, MA) without foetal bovine serum (FBS) and added to HeLa cells in a 24-well culture plate. The cells were incubated for 4 h at 37°C with 5% CO_2. The residual FRET bioprobes and BioPORTER conjugates were removed by washing the cells with culture medium containing 10% FBS. The cells were then incubated for 1 h in the culture medium; subsequently, the culture medium was replaced with serum-free culture medium containing apoptosis-inducing reagents.

2.7. Flow cytometry of HeLa cells

The culture supernatant from the apoptosis-induced HeLa cells was recovered; the cells were then rinsed with 250 μL 0.2 mM EDTA. The chelating solution was removed and combined with the culture supernatant. The remaining cells were incubated with 250 μL each of Accutase and Accumax (Innovative Cell Technologies, Inc., San Diego, CA) cell-detachment mixtures for 10 min at 37°C. The detachment mixtures with the detached cells were added to the whole recovered solution. Trypsin (0.25%; 250 μL) was then added to the culture plate for complete cell detachment. The solutions containing cell debris were combined with those previously recovered and the resulting solutions were filtered and subjected to flow cytometry analysis, using a Flicyme-300 instrument (Mitsui Engineering and Shipbuilding Co., Ltd., Tokyo, Japan). The fluorescence lifetime, fluorescence intensity, and other optical data displayed by the harvested cell population (50,000 cells) were monitored by excitation using a 440-nm semiconductor laser (60 mW). The data obtained was processed using FlowJO software (FlowJO LLC, Ashland, OR).

2.8. Induction of apoptosis in HeLa cells

HeLa cells with internalized bioprobes were incubated in HyClone DMEM/High Glucose culture medium supplemented with 10% FBS for 1 h. The medium was then replaced with FBS-free culture medium. Appropriate amounts of tumour necrosis factor-α (TNF-α; 100 ng/mL) and low (0.5 mg/mL) or high (2 mg/mL)

ACCEPTED MANUSCRIPT

doses of 4-{(2*R*)-2-[(1*S*,3*S*,5*S*)-3,5-dimethyl-2-oxocyclohexyl]-2-hydroxyethyl}piperidine-2,6-dione (cycloheximide) were added to the fresh medium. The treated cells were incubated for 6 h before harvesting for Flicyme analysis. Cells were also collected after 2 and 4 h in the case of the high-dose treatment.

3. Results

Several chimeric FRET bioprobes were prepared for caspase-3 detection (bioprobe-Alexa Fluor 546, bioprobe-Alexa Fluor 594, bioprobe-Alexa Fluor 750, bioprobe-BODIPY 630/650, and bioprobe-QSY 7) using the pUV5casS22tag plasmid and the original unmodified GFP variant, in order to investigate their fluorescence-lifetime components. Fluorescence decay was determined from the TCSPC histograms and good trail-fits were obtained using mono- or multi-exponential decay models. In most cases, well-fitted bi-exponential curves corresponding to unmodified GFP variants and their complexes, were obtained with the various dyes (the decay curves are not shown). Fluorescence lifetime [τ] was defined as the average time that the fluorophore remained in the excited state before returning to ground state by emitting a fluorescence photon. The major τ value of the GFP variant used in this study was 2.6 ns, which was close to previously determined values [47–49]. However, the bioprobes displayed much shorter lifetimes because of their high FRET efficiencies: the fluorescence lifetimes of the complexes containing Alexa Fluor 546, 594, and 750, BODIPY 630/650, and QSY 7 were 0.14, 0.18, 0.65, 0.25, and >> 0.1 ns, respectively. Upon enzymatic digestion, the bioprobes showed decreased FRET efficiency as a result of their conversion into unmodified GFP-like

ACCEPTED MANUSCRIPT

structures through proteolysis (Scheme 1). Therefore, the fluorescence lifetime was observed to increase to 2.6 ns when the activity of caspase-3, a cysteine protease, was investigated *in vitro* using bioprobe-Alexa Fluor 546 and bioprobe-Alexa Fluor 750 under the experimental conditions mentioned in Section 2. Based on the fluorescence decay curves, the bioprobe samples were originally estimated to contain a reasonable quantity of the 2.6-ns component, attributed to the inseparable unmodified-GFP fraction. This amounted to a maximum of 40%, which depended on the kind of fluorescent dye used for modification. Even though we introduced thiol-reactive fluorescent dye derivatives that were supposed to bind to thiol groups equally, their reaction efficiencies fluctuated under the same conditions. However, the bioprobes, fluorescent protein-bound fluorescent dyes, with shorter lifetimes, showed sufficient changes in percentage occupation to facilitate the quantification of FRET increase from the initial unmodified-GFP component without any calibration. Using comparable data processing, the 2.6-ns component present in the bioprobe-Alexa Fluor 546 sample was found to increase from 14% to 73% during proteolysis. A similar change (from 40% to 98%) was observed for bioprobe-Alexa Fluor 750 (Fig. 1). These results show that the measured fluorescence lifetimes of the FRET bioprobes have greater applicability in quantitative assays of biological events compared to ordinary FRET measurements. Moreover, Alexa Flour 750 is a fine acceptor molecule, free from supposed compensation, which would facilitate the expedient and direct use of our system for high-throughput assays.

Having demonstrated the evaluation of FRET bioprobes *in vitro*, the probes were introduced into cells and their fluorescence lifetime within the cells was measured statistically using Flicyme. A verified GFP variant for

ACCEPTED MANUSCRIPT

caspase-3 monitoring [15] and an additional variant for caspase-9 sensing were constructed; these fluorescence proteins were modified with selected dyes. The modified proteins were then incorporated into cells using the BioPORTER reagent as per the manufacturer instructions. Flicyme analysis measures the average fluorescence lifetimes of all components within each cell within a population; therefore, we attempted to use cells in a steady state for all analyses, to maintain a constant cell microenvironment and account for the sensitivity of fluorescence lifetime to various factors such as ionic strength, pH, or temperature [25, 26]. Eventually, DyLight 680 (bioprobe for caspase-9) and Alexa Fluor 750 (bioprobe for caspase-3) were selected as acceptor molecules. This was further ascribed to the relative robustness of the bioprobes' fluorescence lifetime absolute values, as a result of the inevitable fluctuations in cellular conditions. DyLight 680 is also ideal for FRET-based high-throughput analysis compared with calibration-free Alexa Fluor 750, described above. Following the incorporation of bioprobes into the cells, the simple diffusion capacity of the probes was analysed by determining the quantity of expressed proteins within the cells by microscopic analysis [15]. For this purpose, apoptosis was induced, by the action of chemical reagents, in pre-treated cells; the cells were subsequently harvested, as described in Section 2. The cells were then analysed using Flicyme. The obtained data was processed using FlowJO software and analysed by careful gating (Supplementary Fig. S2). Firstly, parameters were set for the intensity thresholds of the donor and acceptor fluorescence, in order to eliminate cell populations that demonstrated no uptake of bioprobes. The fluorescence lifetime distributions of the gated cell populations were then explored and the results were plotted as representative histograms (Fig. 2). Time-point

ACCEPTED MANUSCRIPT

data for the lifetime distribution of the bioprobes for caspase-9 and caspase-3 obtained from the histograms, demonstrated time-dependent shifts toward longer fluorescence lifetimes (Fig. 2A). Dose-response data for the fluorescence-lifetime distributions of the bioprobes also exhibited comparable shifts to longer fluorescence lifetimes (Fig. 2B). The longer lifetimes implied a progress in FRET cancellations upon protease activation. The shift patterns of the histograms were very similar; however, absolute time or dose dependencies of the apoptotic responses were observed for all trials. The shift patterns of the respective enzymes were compared in greater detail by calculating the median values of the fluorescence lifetimes from individual histograms for 3 experimental runs. The median, and not the mean values exemplify the distinctive feature of populations during the handling of such asymmetric histograms. The average of median values obtained from 3 histograms were plotted as a function of time or dose (Fig. 3). Caspase-9 activation was relatively reproducible and was almost saturated within 2 h, remaining constant thereafter. On the other hand, caspase-3 activation varied for each experiment; however, the activation was generally initiated at around 2 h and proceeded gradually (Fig. 3A). The dose-dependency histograms (Fig. 3B) appeared to show oscillations in caspase-9 activation upon treatment with various quantities of inducers. The extent of caspase-3 activation appeared to show a closer relationship to the dose. Relatively large errors in processed data for each distinct parameter response during apoptotic activity (Fig. 3) may indicate actual oscillation in each cell. This suggests that the relationship between 2 significant apoptotic proteases could be interpreted by high-throughput measurement of the fluorescence lifetimes of FRET bioprobes, similar to the analysis of the corresponding performances by

ACCEPTED MANUSCRIPT

live-cell imaging, rather than using the usual bulk assay.

4. Discussion

Statistical, versatile, and specific assays of cellular events are essential tools for omics studies and drug development; therefore, there is a continuous increase in the demand for such assays. In this study therefore, we developed a combination of high-throughput assay and dynamic characterization of living cells. Our aim was to establish an advanced system for dynamic studies of various cell populations. This method was applied for high-throughput analysis of apoptosis-induction processes, using a varied signal transduction model. In order to ensure the reliability and ease-of-use of our system, robust and sensitive FRET-based, chimeric sensing molecules, or chimeric FRET bioprobes, were prepared and applied to a fluorescence-lifetime detection apparatus. Each chimeric FRET bioprobe consisted of a fluorescent protein linked to an organic dye through a covalent bond; while afforded ease of replacing the dye [30] and thus, we demonstrated control of fluorescence lifetime by an appropriate choice of dye. The fluorescence lifetimes of chimeric FRET bioprobes were shown, by *in vitro* experiments, to be suitable for use in quantitative monitoring of biological events. Furthermore, different bioprobes with distinctive fluorescence properties for different targets were believed to display independent fluorescence lifetimes (despite being in a mixture), allowing for their use as discriminatory sensor molecules in mixed samples. The developed FRET bioprobes are also useful as normalized sensor molecules. These features prompted the comparison of divergent phenomena in cellular dynamics using various FRET

ACCEPTED MANUSCRIPT

bioprobes (simultaneously).

The chimeric nature of the bioprobes permits a wide choice of components; therefore, bioprobes that are not overly affected by cell conditions during the measurement of their fluorescence lifetimes can be conducted for cell-based experiments. The apparatus employed in this study for lifetime measurements, Flicyme, delivered average fluorescence lifetimes for single cells; therefore, we constructed histograms depicting the distributions of fluorescence lifetimes in significant cell populations stimulated to undergo apoptosis by drug treatment, after gating with fluorescence intensities. We observed shifts in the histograms corresponding to longer fluorescence lifetimes, which could be attributed to dose- and time-dependent cancellation of FRET. We selected median values (rather than mean) for all further population analyses because of the asymmetry of the resulting histograms. Thus, we determined the median values from 3 repeated runs, as shown in Fig. 3. Subtle distinctions in dose-dependencies were observed between the two caspases (Fig. 3B). This appeared to indicate greater oscillation, especially in the case of caspase-9 activation, upon treatment with various amounts of inducers. The extent of caspase-3 activation was directly dependent on the dose. The time-dependence of caspase activation was recognizable for caspase-9, but not for caspase-3 (at the same stage). We previously demonstrated that multiplications of caspase-9 enhanced levels and their duration programmed times to activate caspase-3 that were average in 3 h after apoptotic induction we introduced here (unpublished data). So unique factor seemed to be much fluctuated in a cell. Consequently, activation characteristics of the 2 caspases (identified in this study) upon induction of apoptosis appeared to be consistent with their different roles (as a

ACCEPTED MANUSCRIPT

mediator or as an executor) in the signalling pathway [33–38]. Therefore, we suggest that coupling of the chimeric FRET bioprobes and high-throughput fluorescence lifetime measurements might provide a reliable system for the evaluation of cellular signal transduction. The use of these FRET bioprobes could also be extended to new targets; therefore, this system could be utilized as a conventional cell-based assay in the future.

5. Conclusions

The dynamic responses of cell populations to agents that stimulate apoptotic signal transduction were quantitatively and statistically analysed. This was achieved by a combination of flow cytometry and fluorescence-lifetime measurements of FRET bioprobes within cells; the FRET-based sensing molecules targeted various cellular events and the currently established component technologies were carefully compared and adjusted. The main objective of this study was to confirm the effectiveness of a novel analytical method developed using the advances in both HTP and HCS systems, and the results obtained achieved this purpose. Furthermore, this system could be applied to versatile signal transduction pathways. Therefore, we conclude that the system developed in this study could be applied as a common approach.

ACCEPTED MANUSCRIPT

Acknowledgements

We would like to thank Mr. Shigeyuki Nakata, Mr. Hironori Hayashi, and Ms. Yumi Asano of Mitsui Engineering and Shipbuilding Co. Ltd. for their technical support.

ACCEPTED MANUSCRIPT

References

[1] A. Yano, S. Oda, T. Fukami, M. Nakajima, T. Yokoi, Development of a cell-based assay system considering drug metabolism and immune- and inflammatory-related factors for the risk assessment of drug-induced liver injury, Toxicol. Lett. 228 (2014)13-24.

[2] R. Edmondson, J.J. Broglie, A.F. Adcock, L. Yang, Three-dimensional cell culture systems and their applications in drug discovery and cell-based biosensors, Assay Drug Dev. Technol. 12 (2014) 207-218.

[3] M.J. Wawer, K. Li, S.M. Gustafsdottir, V. Ljosa, N.E. Bodycombe, M.A. Marton, K.L. Sokolnicki, M.A. Bray, M.M. Kemp, E. Winchester, B. Taylor, G.B. Grant, C.S. Hon, J.R. Duvall, J.A. Wilson, J.A. Bittker, V. Dančík, R. Narayan, A. Subramanian, W. Winckler, T.R. Golub, A.E. Carpenter, A.F. Shamji, S.L. Schreiber, P.A. Clemons, Toward performance-diverse small-molecule libraries for cell-based phenotypic screening using multiplexed high-dimensional profiling, Proc. Natl. Acad. Sci. USA 111 (2014) 10911-10916.

[4] A.B. Lyons, C.R. Parish, Determination of lymphocyte division by flow cytometry, J. Immunol. Methods 171 (1994) 131-137.

[5] K.E. Howard, I.L. Fisher, G.A. Dean, M. Jo Burkhard, Methodology for isolation and phenotypic characterization of feline small intestinal leukocytes, J. Immunol. Methods 302 (2005) 36-53.

[6] G. Freer, L. Rindi, Intracellular cytokine detection by fluorescence–activated flow cytometry:basic principles and recent advances, Methods 61 (2013) 30-38.

[7] H.T. Maecker, Multiparameter flow cytometry monitoring of T cell responses, Methods in Mol. Biol. 485

ACCEPTED MANUSCRIPT

(2009) 375-391.

[8] H.J. Mayerson, A practical approach to the flow cytometric detection and diagnosis of T-cell lymphoproliferative disorders, Laboratory Hematology 16 (2010) 32-52.

[9] G. Freer, Intracellular staining and detection of cytokines by fluorescence-activated flow cytometry, Methods Mol. Biol. 1172 (2014) 221-234.

[10] J.T. Wessels, K. Yamauchi, R.M. Hoffman, F.S. Wouters, Advances in cellular, subcellular, and nanoscale imaging in vitro and in vivo, Cytometry A 77 (2010) 667-676.

[11] C. Radu, H.S. Adrar, A. Alamir, I. Hatherley, T. Trinh, H. Djaballah, Designs and concept reliance of a fully automated high-content screening platform. J. Lab. Autom. 17 (2012) 359-369.

[12] M. Haller, E. Bier, P.C. DeRose, G.A. Cooksey, S.J. Choquette, A.L. Plant, J.T. Elliott, An automated protocol for performance benchmarking a widefield fluorescence microscope, Cytometry A (2014) doi:10.1002/cyto.a.22519

[13] C.R. Thoma, M. Zimmermann, I. Agarkova, J.M. Kelm, W. Krek, 3D cell culture systems modeling tumor growth determinants in cancer target discovery, Adv. Drug Deliv. Rev. 69-70 (2014) 29-41.

[14] M. Suzuki, Y. Ito, E.H. Savage, Y. Husimi, K.T.n Douglas, Protease-sensitive signaling by chemically engineered intramolecular fluorescent resonance energy transfer mutants of green fluorescent protein, Biochim. Biophys. Acta. 1679 (2004) 222-229.

[15] M. Suzuki, Y. Ito, I. Sakata, T. Sakai, Y. Husimi, K.T. Douglas, Caspase-3 sensitive signaling in vivo in

ACCEPTED MANUSCRIPT

apoptotic HeLa cells by chemically engineered intramolecular fluorescence resonance energy transfer mutants of green fluorescent protein, Biochem. Biophys. Res. Commun. 330 (2005) 454-460.

[16] A. Miyawaki, Visualization of the spatial and temporal dynamics of intracellular signaling, Dev. Cell 4 (2003) 295-305.

[17] B.H. Hou, H. Takanaga, G. Grossmann, L.Q. Chen, X.Q. Qu, A.M. Jones, S. Lalonde, O. Schweissqut, W. Wiechert, W.B. Frommer, Optical sensors for monitoring dynamic changes of intracellular metabolite levels in mammalian cells, Nat. Protoc. 6 (2011) 1818-1833.

[18] C.F. Kaminski, E.J. Rees, G.S. Schierie, A quantitative protocol for intensity-based live cell FRET imaging, Methods Mol. Biol. 1076 (2014) 445-454.

[19] E. Galperin, V.V. Verkhusha, A. Sorkin, Three-chromophore FRET microscopy to analyze multiprotein interactions in living cells. Nat. Methods 1 (2004) 209-217.

[20] D.R. Matthews, G.O. Fruhwirth, G. Weitsman, L.M. Carlin, E. Ofo, M. Keppler, P.R. Barber, I.D. Tullis, B. Vojnovic, T. Ng, S.M. Ameer-Beg, A multi-functional imaging approach to high-content protein interaction screening, PLoS One 7 (2012) e33231.

[21] T. Su, S. Pan, Q. Luo, Z. Zhang, Monitoring of dual bio-molecular events using FRET biosensors based on mTagBFP/sfGFP and mVenus/mKOk fluorescent protein pairs, Biosens. Bioelectron 46 (2013) 97-101.

[22] J. Korczynski, J. Wlodarczyk, Fluorescence lifetime imaging microscopy (FLIM) in biological and medical research, Postepy. Biochem. 55 (2009) 434-440.

ACCEPTED MANUSCRIPT

[23] H. Wallrabe, A. Periasamy, Imaging protein molecules using FRET and FLIM microscopy, Curr. Opin. Biothechnol. 16 (2005) 19-27.

[24] S. Padilla-Parra, N. Audugé, H. Lalucque, J.C. Mevel, M. Coppey-Moisan, M. Tramier, Quantitative comparison of different fluorescent protein couples for fast FRET-FLIM acquisition, Biophys. J. 97 (2009) 236

[25] M. Martin-Fernandez, S.V. Longshaw, I. Kirby, G. Santis, M.J.Tobin, D.T. Clarke, G.R. Jones, Adenovirus type-5 entry disassembly followed in living cells by FRET, fluorescence anisotropy and FLIM, Biophys. J. 87 (2004) 1316-1327.

[26] K. Suhling, J.A. Levitt, P.H. Chung, M.K. Kuimova, G. Yahioglu, Fluorescence lifetime imaging of molecular rotors in living cells, J. Vis. Exp. 60 (2012) pii:2025.

[27] P. Nagy, L. Bene, W.C. Hyun, G. Vereb, M. Braun, C. Antz, J. Paysan, S. Damjanovich, J.W. Park, J. Szollsi, Novel calibration method for flow cytometric fluorescence resonance energy transfer measurements between visible fluorescent proteins, Cytometry A 67 (2005) 86-96.

[28] X. Wu, J. Simone, D. Hewgill, R. Siegel, P.E. Lipsky, L. He, Measurement of two caspase activities simultaneously in living cells by a novel dual FRET fluorescent indicator probe, Cytometry A 69 (2006) 477-486.

[29] R. Fox, M. Aubert, Flow cytometric detection of activated caspase-3. Methods Mol. Biol. 414 (2008) 47-56.

[30] M. Suzuki, S. Tanaka, Y. Ito, M. Inoue, T. Sakai, K. Nishigaki, Simple and tunable förster resonance

ACCEPTED MANUSCRIPT

energy transfer-based bioprobes for high-throughput monitoring of caspase-3 activation in living cells by using flow cytometry, Biochim. Biophys. Acta. MCR 1823 (2012) 215-226.

[31] W. Zhang, M. Suzuki, Y. Ito, K.T. Douglas, A Chemically modified green-fluorescent protein that responds to cleavage of an engineered disulphide bond by fluorescence resonance energy transfer (FRET)-based changes, Chem. Lett. 34 (2005) 766-767.

[32] T. Kihara, C. Nakamura, M. Suzuki, S.W. Han, K. Fukazawa, K. Ishihara, J. Miyake, Development of a method to evaluate caspase-3 activity in a single cell using a nanoneedle and a fluorescent probe, Biosens. Bioelectron 25 (2009) 22-27.

[33] J.T. Pai, M.S. Brown, J.L. Goldstein, Purification and cDNA cloning of a second apoptosis-related cysteine protease that cleaves and activates sterol regulatory element binding proteins, Proc. Natl. Acad. Sci. USA 93 (1996) 5437-5442.

[34] H.S. Choi, S. Han, H. Yokota, K.H. Cho, Coupled positive feedbacks provoke slow induction plus fast switching in apoptosis, FEBS. Lett. 581 (2007) 2684-2690.

[35] C. Maueröder, R.A. Chaurio, S. Platzer, L.E. Muño, C. Berens, Model systems for rapid and slow induction of apoptosis obtained by inducible expression of pro-apoptotic proteins, Autoimmunity 46 (2013) 329-335.

[36] R. Kim, M. Emi, K. Tanabe, Role of mitochondria as the gardens of cell death, Cancer Chemother. Pharmacol. 57 (2006) 545-553.

ACCEPTED MANUSCRIPT

[37] I.N. Lavrik, Systems biology of death receptor networks: live and let die, Cell Death Dis. 5 (2014) e1259.

[38] S.W. Ryter, K. Mizumura, A.M. Choi, The impact of autophagy on cell death modalities, Int. J. Cell Biol. 2014 (2014) 502676.

[39] A. Rasul, M. Khan, M.Ali, J. Li, X. Li, Targeting apoptosis pathways in cancer with alantolactone and isoalantolactone, Scientific World Journal 2013 (2013) 248532.

[40] S. Zhang, M. Yu, H. Deng, G. Shen, Y. Wei, Polyclonal rabbit anti-human ovarian cancer globulins inhibit tumor growth through apoptosis involving the caspase signaling, Sci. Rep. 4 (2014) 4984.

[41] E.J. Sohon, M.J. Shin, D.W. Kim, E.H. Ahn, H.S. Jo, D.S. Kim, S.W. Cho, K.H. Han, J. Park, W.S. Eum, H.S. Hwang, S.Y. Choi, Tat-fused recombinant human SAG prevents dopaminergic neurodegeneration in a MPTP-induced Parkinson's disease model, Mol.Cells 37 (2014) 226-233.

[42] G. Wendt, V. Kemmei, C. Patte-Mensah, B. Uring-Lambert, A. Eckert, M.J. Schmitt, A.G. Mensah-Nyangan, Gamma-hydroxybutyrate, acting through an anti-apoptotic mechanism, protects native and amyloid-precursor-protein-transfected neuroblastoma cells against oxidative stress-induced death, Neuroscience 263 (2014) 203-215.

[43] Z. Qualls, D. Brown, C. Raminochansingh, L.L. Hurley, Y. Tozabi, Protective effects of curcumin against rotenone and saisolinol-induced toxicity implications for Parkinson's disease, Neurotox. Res. 25 (2014) 81-89.

[44] B. Fadeel, Z. Hassan, E. Hellström-Lindberg, JI Henter, S. Orrenius, B. Zhivotovsky, Cleavae of Bcl-2 is an early event in chemotherapy-induced apoptosis of human meyloid leukemia cells, Leukemia. 13 (1999)

ACCEPTED MANUSCRIPT

719-728.

[45] J. Liu, Y. Yao, H. Ding, R. Chen, Oxymatrine triggers apoptosis by regulating Bcl-2 family proteins and activating caspase-3/caspase-9 pathway in human leukemia HL-60 cells, Tumour Biol. 35 (2014) 5409-5415.

[46] M.L. Wurstle, M.Rehm, A systems biology analysis of apoptosome formation and apoptosis execution supports allosteric procaspase-9 activation, J. Biol. Chem. 289 (2014) 26277-26289.

[47] R. Swaminathan, C.P. Hoang, A.S. Verkman, Photobleaching recovery and anisotropy decay of green fluorescent protein GFP-S65T in solution and cells: cytoplasmic viscosity probed by green fluorescent protein translational and rotational diffusion, Biophys. J. 72 (1997) 1900-1907.

[48] A. Sacchetti, R. Cioccocioppo, S. Alberti, The molecular determinants of the efficiency of green fluorescent protein mutants, Histol. Histopathol. 15 (2000) 101-107.

[49] A.J. Visser, S.P. Laptenok, N.Y. Visser, A. van Hoek, D.J. Birch, J.C. Brochon, J.W. Borst, Time-resolved FRET fluorescence spectroscopy of visible fluorescent protein pairs, Eur. Biophys. J. 39 (2010) 241-253.

ACCEPTED MANUSCRIPT

ACCEPTED MANUSCRIPT

Footnotes

[1]Abbreviations used

HTP, high-throughput screening, HCS, high-content screening, FRET, fluorescence resonance energy transfer, FACS, fluorescence activated cell sorter, GFP, green fluorescent protein, PBS, phosphate buffered saline, DTT, dithiothreitol, HEPES, 2-[4-(2-hydroxyethyl)piperazin-1-yl] ethanesulfonic acid, PIPES, 1,4-Piperazinediethanesulfonic acid, TCSPC, time-correlated single-photon counting, CHAPS, 3-[(3-Cholamidopropyl)dimethylammonio]-1-propanesulfonate,FBS, fetal bovine serum, TNF, tumor necrosis factor

ACCEPTED MANUSCRIPT

ACCEPTED MANUSCRIPT

Figure Legends

Scheme 1. The mechanism of protease sensing by chimeric FRET bioprobes. FRET occurs between a green fluorescent protein and an organic dye containing a bioprobe. The protease recognition sequence is located between the GFP and the binding site for the dye; therefore, FRET disappears when the dye is released from the fluorescent protein, along with the digested protein fragments.

Fig. 1. Fluorescence lifetime component analysis upon treatment with caspase-3. Chimeric FRET bioprobes for caspase-3, which utilised GFP as the donor and AlexaFluor 546 or AlexaFluor 750 as the acceptor molecule, were incubated in an assay buffer with or without 1 U caspase-3 at 30°C for 2 h. The fluorescence lifetime of each of the reaction products was measured using a MicroTime-200 (with excitation) at 470 nm; the results were analysed to fit one of several fluorescence-lifetime exponential decay curves (representative results from 3 independent trials are shown here).

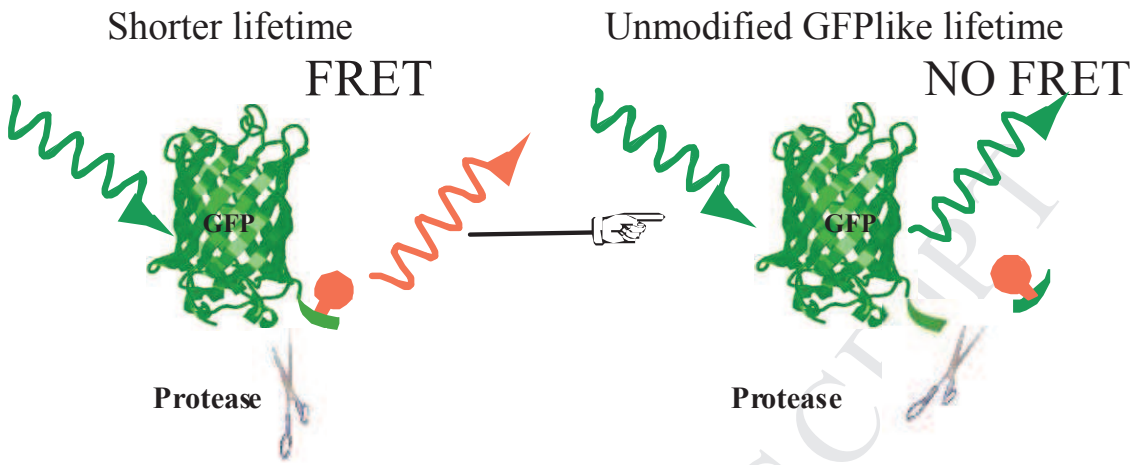
Fig. 2. (A) Time-dependent profiles of fluorescence lifetime distributions upon induction of apoptosis. HeLa cells containing FRET bioprobes for caspase-3 (left) or caspase-9 (right), were treated with 100 ng/mL TNF-α and 2 mg/mL cycloheximide (in order to induce apoptosis) and subsequently cultured for 2 h (blue) or 4 h (green). The cells were harvested and subjected to flow cytometry to determine the fluorescence-lifetime

ACCEPTED MANUSCRIPT

distributions of individual cell populations. Untreated HeLa cells were also harvested and subjected to a similar analysis (red, control). (B) Reagent-dose dependency of the fluorescence lifetime distribution upon induction of apoptosis. HeLa cells, containing the appropriate FRET bioprobes for caspase-3 (left) or caspase-9 (right), were treated with 100 ng/mL TNF-α and 0.5 mg/mL (low dose, blue) or 2 mg/mL (high dose, green) cycloheximide for 6 h to induce apoptosis. Cells were harvested for flow cytometric analysis. Untreated cells were also examined (red).

Fig. 3. (A) Time-dependent shifts in the median values of the fluorescence lifetime distributions of HeLa cell populations containing caspase-3-sensing (right) or caspase-9-sensing (left) bioprobes. The median values of the fluorescence-lifetime distributions obtained from Fig. 3A (from 3 experiments) were plotted as a function of time. (B) Reagent dose-dependency of the changes in the median values of fluorescence-lifetime distributions of HeLa cell populations containing the caspase-3-sensing (right) or caspase-9-sensing (left) bioprobes. The median values of the fluorescence-lifetime distributions from Fig. 3B (from 3 experiments) are displayed for each dose.

ACCEPTED MANUSCRIPT



Scheme 1

ACCEPTED MANUSCRIPT

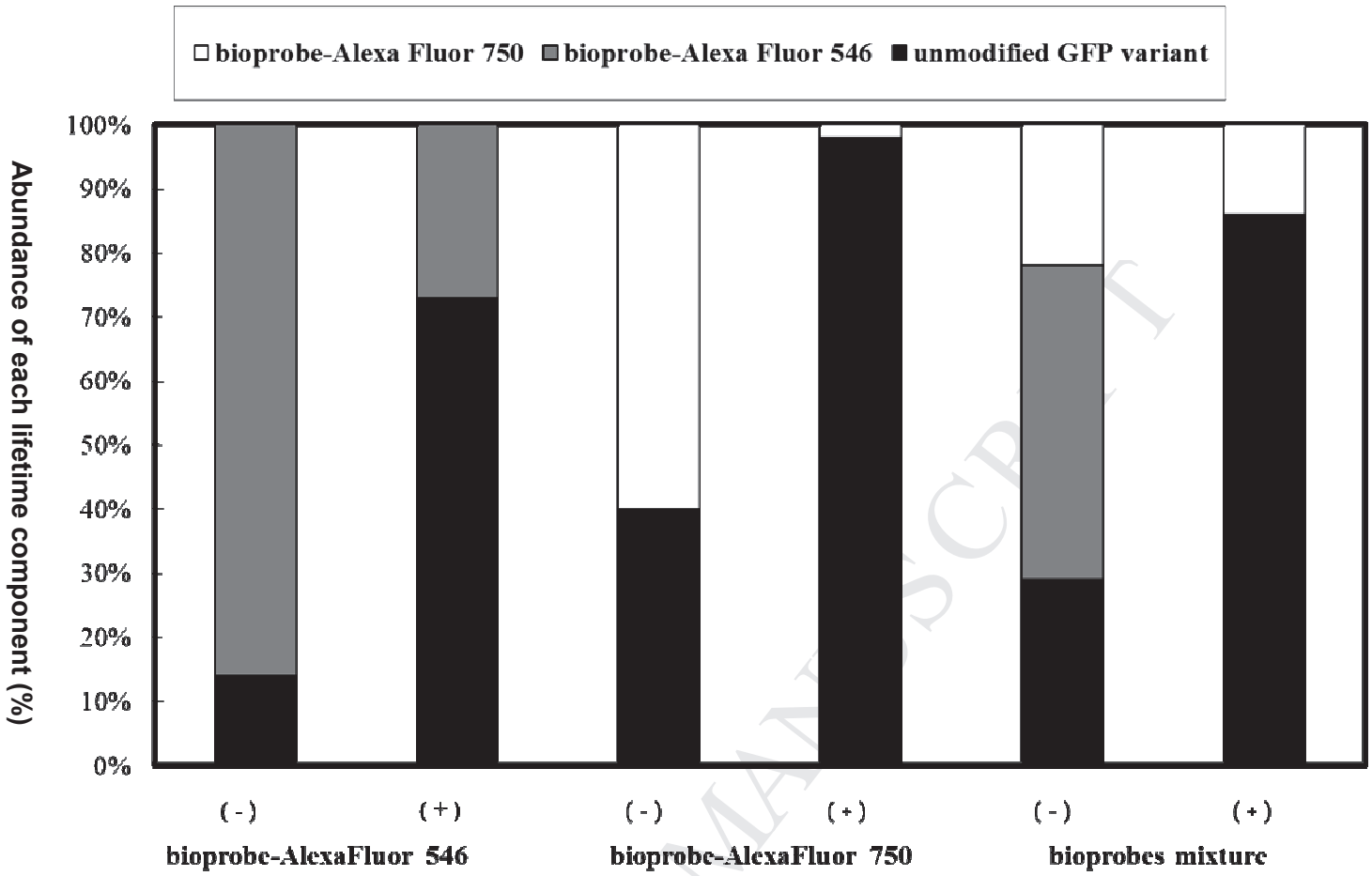


Fig. 1

ACCEPTED MANUSCRIPT

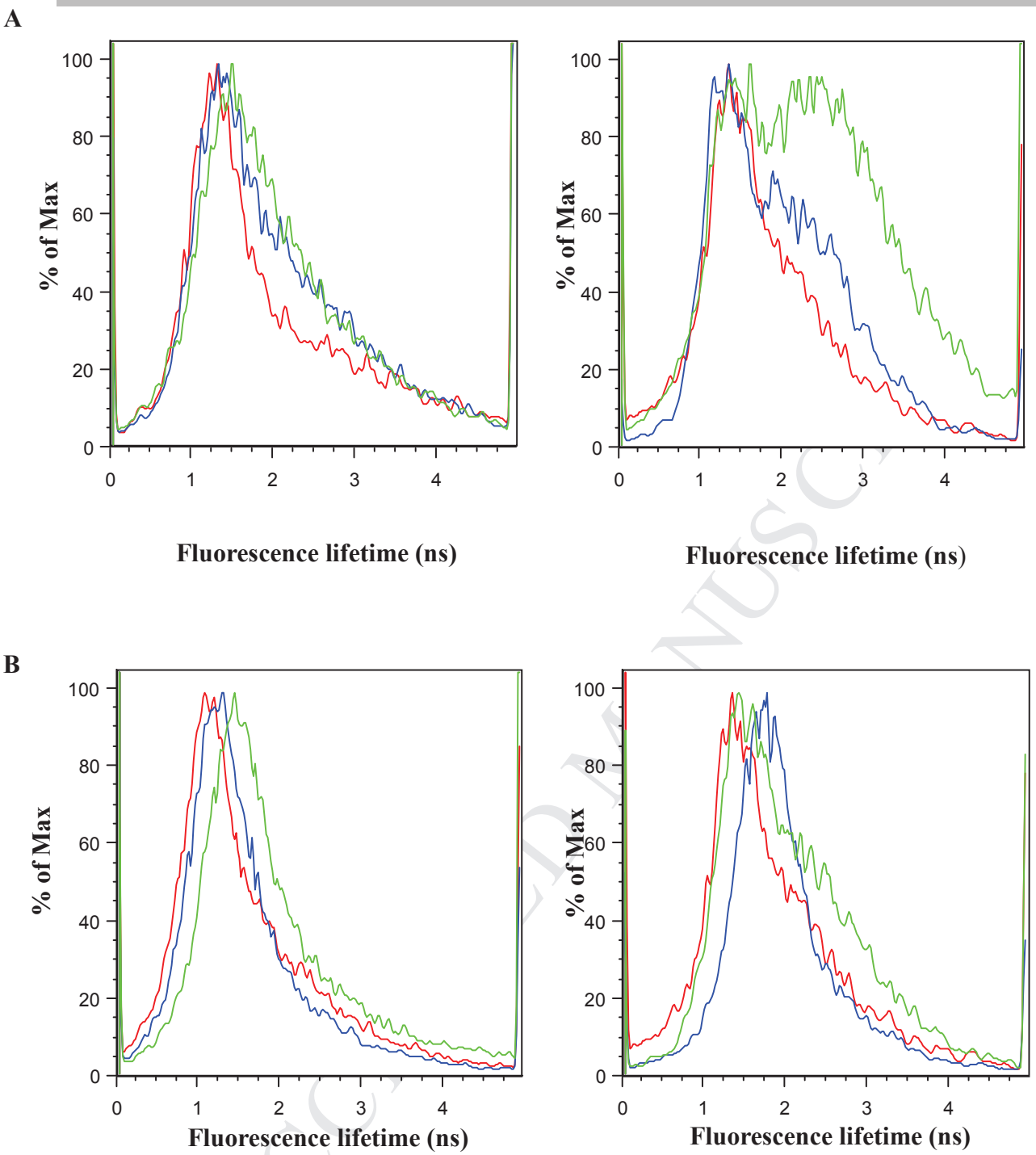
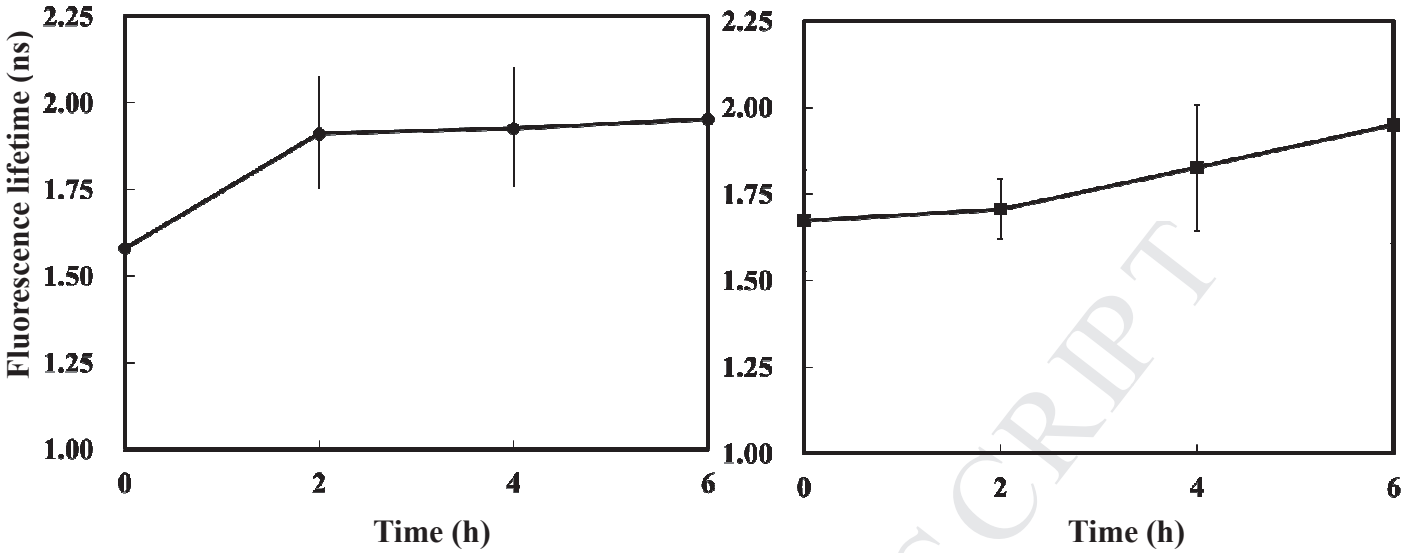
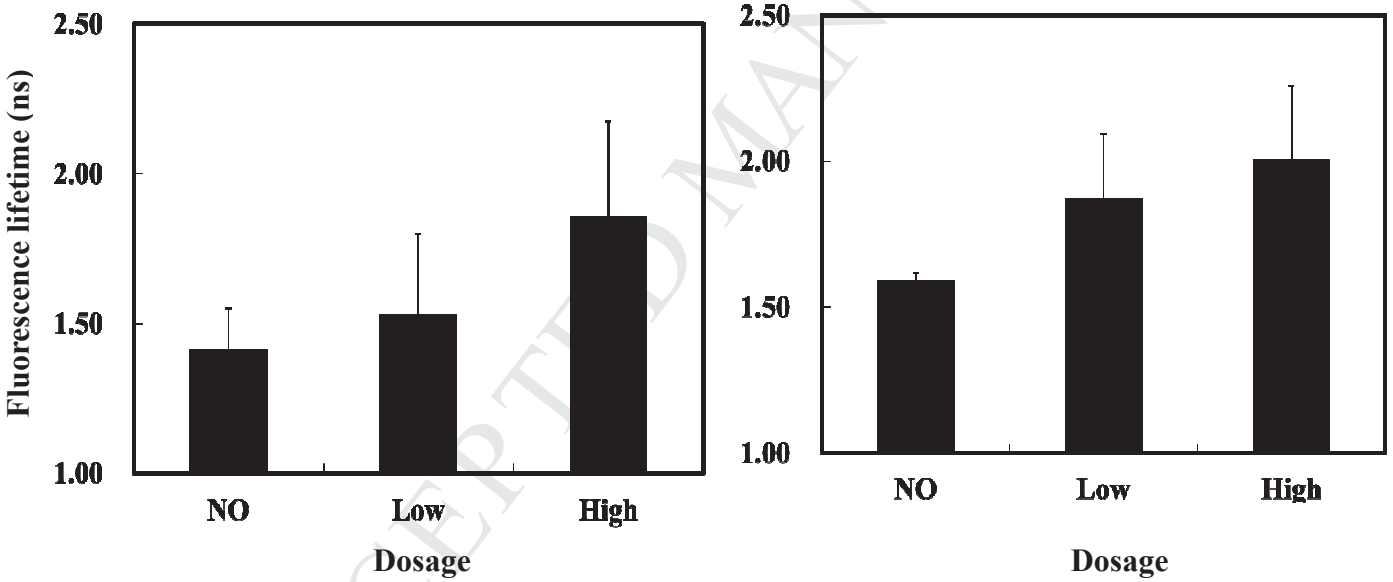

A
100
80
60
40
20
0
% of Max
0
1
2
3
4
Fluorescence lifetime (ns)
B
100
80
60
40
20
0
% of Max
0
1
2
3
4
Fluorescence lifetime (ns)

Fig. 2

A



B



ACCEPTED MANUSCRIPT

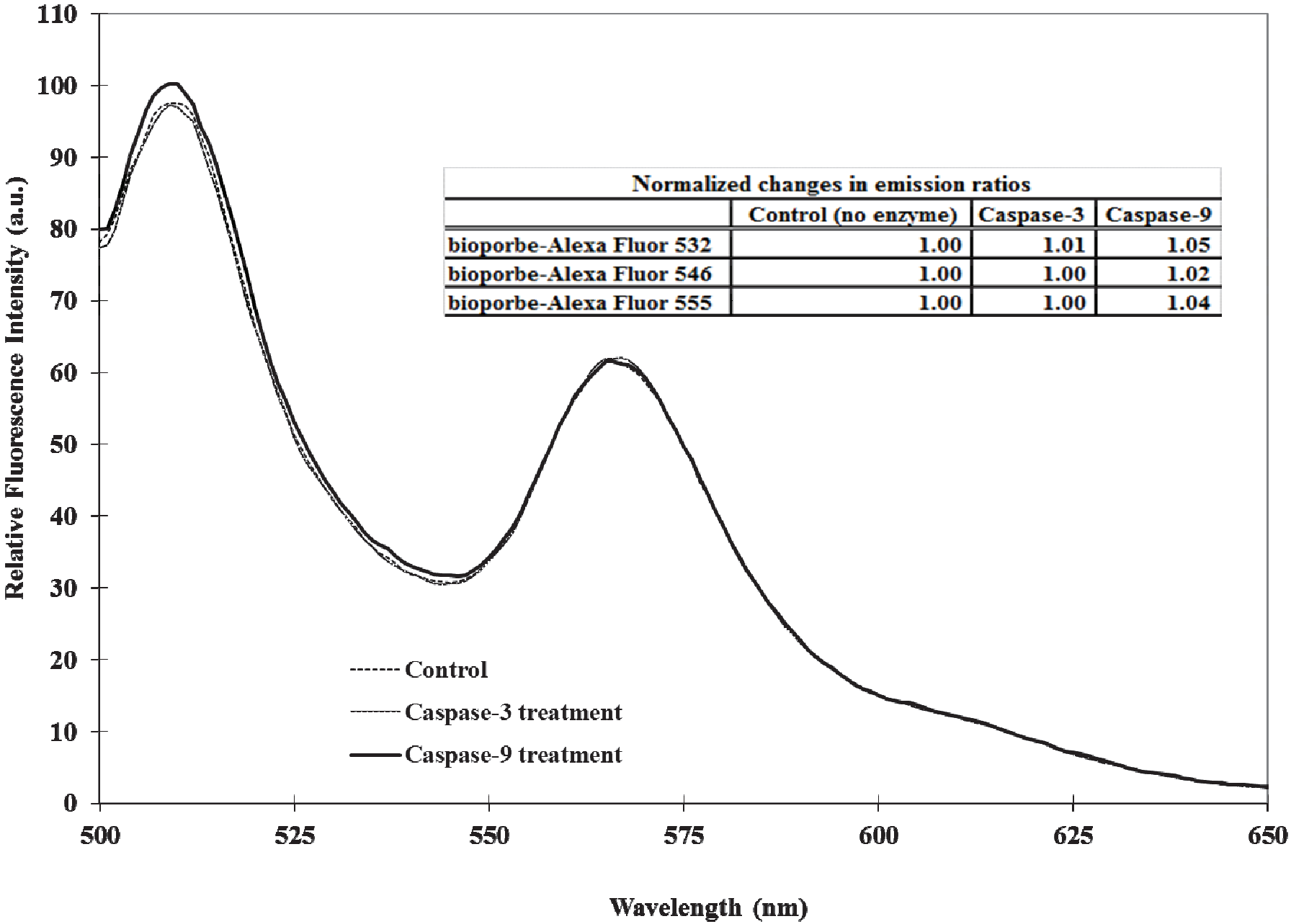
Fig. 3

ACCEPTED MANUSCRIPT

Supplementary Fig. S1.Changes in the emission patterns of bioprobe-Alexa Fluor 555 on *in vitro* treatments with caspase-3 or caspase-9. Emission profiles in the presence of caspase-3 (thin line) or caspase-9 (thick line) or absence of caspase (dashed line) were assessed. We normalized emission ratios (dye emission maximum/fluorescent protein emission maximum) in the absence of caspase as 1 and calculated emission ratios in the presence of caspase-3 or caspase-9. FRET cancellation due to enzymatic digestion were represented by values over 1 (in set table). We tried this evaluation twice in every cases.

ACCEPTED MANUSCRIPT

ACCEPTED MANUSCRIPT



Normalized changes in emission ratios			
	Control (no enzyme)	Caspase-3	Caspase-9
bioporbe-Alexa Fluor 532	1.00	1.01	1.05
bioporbe-Alexa Fluor 546	1.00	1.00	1.02
bioporbe-Alexa Fluor 555	1.00	1.00	1.04

ACCEPTED MANUSCRIPT

Supplementary Fig. S2. Gating scheme for fluorescence-lifetime distribution analysis. The non-fluorescent cell population was identified to facilitate the extraction of the fluorescent/bioprobe-introduced cell population, by enclosing the non-bioprobe-introduced cells (dot-plot figure on the left) in a discriminatory gate. The bioprobe-introduced cell population, or the population existing outside the border of the non-bioprobe-introduced cell gate, was then successfully estimated (dot-plot figure in the middle). The single cell average fluorescence-lifetime for each cell population was calculated using the histograms depicting the individual fluorescence-lifetime distributions (histograms on the right).

ACCEPTED MANUSCRIPT

ACCEPTED MANUSCRIPT

Gating scheme for fluorescence-lifetime distribution analysis

